

# High Gain Metamaterial Implemented Antenna Design with Circular Polarization for mm-Wave 5G and 6G Sub-THz Communication

# Aafreen Khan<sup>1</sup>, AnwarAhmad<sup>1</sup> Maksud Alam<sup>2</sup>

<sup>1</sup>Department of Electronics and Communication Jamia Millia Islamia, New Delhi, India.

<sup>2</sup>Department of Electronics and Communication, Galgotia college of engineering and technology, Greater Noida, India.

**E-mail:** ¹aafreen.khan1994@gmail.com, ¹aahmad4@jmi.ac.in, ²alam.maksud@gmail.com.

### **Abstract**

A high-gain metamaterial-enabled circularly polarized antenna has been proposed. Two patch structures patch A and patch B have been designed by using different shape slots. After slot etching on the patch, two different metamaterial techniques were used. Circular metamaterial (MTM) was implemented for Patch A, while rectangular MTM was used for Patch B. The implementation of MTM resulted in increased antenna gain, as well as improvements in impedance bandwidth RL and AR. So, in the proposed article two antenna structures ANT-A and ANT-B, are presented. The maximum gain achieved for ANT-A is 34.759dBi, covering the frequency bands (28.997-202.113) GHz, and (205.884-336.693) while in the case of ANT-B, it is 36.3155dBi, covering the frequency bands (29.178-330.490) GHz, and (334.936-336.702) GHz. The proposed antenna structure is a useful design for mm-wave 5G and 6G Sub-THz communications.

**Keywords:** CP, AR, MTM, Sub-THz, mm-Wave

### 1. Introduction

High gain and large bandwidth antennas are preferred at millimetre--wave (mm-Wave) frequencies to achieve a high data rate and to nullify the absorption of electromagnetic waves (EM) waves due to the atmosphere at higher frequency bands. Similarly, for sub-terahertz (Sub-THz) frequency bands, high-gain antennas are essential for long-distance communications. Among various antenna types, microstrip patch antennas find widespread applications due to their lightweight and ease of design. However, designing microstrip patch antennas with high-gain characteristics is challenging for mm-wave and sub-THz applications. So, here in the proposed design, the high gain antenna including a slot loaded with MTM(Metamaterial) implementation has been designed with the good RL BW (Return loss Bandwidth) along with the circularly polarized frequency bands at the mm-wave and Sub-THz bands.

### 2. Related Work

Various types of improvements on microstrip patch antenna have been presented in recent studies. These enhancements include antenna miniaturization and multi-resonant wide band characteristics using slotted microstrip with modified ground plane [1]. A triband antenna consisting of two long-side monopoles and the double-sided square dipole array for 1G, 5G, and Wi-Fi access applications has been shown in [2]. In [3] the periodic fractal parasitic structure (PFPS) has been used along with the patch to get the circularly polarized (CP) performance. For mm-wave applications, circularly polarized antenna illustrates the CP and wideband characteristics with maximum gain of 10dBic [4]. In the S-shaped dipole array, four S-shaped patches have been used and the good impedance bandwidth and the maximum gain of 18.5dBic have been achieved [5]. In the meander line loaded cp polarized antenna for C band applications, good AR bandwidth has been achieved by the implementation of a meander line and inverted-L-shaped grounded strip [6]. In [7] transmit array is used for CP polarization, achieving a peak gain of 26.4dBi with a low-cost design. A substrate integrated waveguide (SIW) slot array mm-wave antenna, covering the band (28–32 GHz), exhibits good gain and miniatured size characteristics [8] [8]. In the 3D printed radar antenna for K band applications, the gain achieved is 18.3dBi with a bandwidth of 2.2GHz [9]. In [10] three slotted SIW antenna elements are given with different radiators and good return loss bandwidth and ARBW (Axial Ratio Bandwidth) has been achieved with a directivity of 14dBi. In a double Xi-shaped mmwave antenna the frequency band covered is (24.7-27.7) GHz and the peak gain value is

19.2dBi [11]. In a 60 GHz array structure for 5G applications, a low-cost compact structure has been designed with a peak gain of 12.4dBi [16]. In a 5G MIMO dipole small cell antenna, the maximum gain achieved is 9.2dBi [17].

In the circularly polarized open slot antenna for mm-wave and sub-mm-wave systems, a simple structure has been proposed, along with a good axial ratio (AR) bandwidth of less than 3dB [12]. [12]. CP polarized antennas for the mm-wave frequency band have been studied in [13-14]. In [15], enhancement in the gain by 1.5dBi has been achieved by using negative permeability metamaterial on low temperature co-fired ceramic (LTCC) substrate. The proposed antennas, A and B, achieves high gain, high bandwidth, and CP properties and are useful in for 5G mm-wave and Sub-THz applications.

### 3. Proposed Work

The proposed antenna, has been designed on a Taconic CER-10 substrate with a permittivity of 10 and height of 0.7mm. The front view of the proposed antenna structure is given in Figures 1(a) and (b). The lower layer of ground has dimensions of 5.141mm× 5.883mm, and the upper layer, called a patch, has a rectangle shape of size 0.941mm×1.68mm. The schematic of a simple rectangle shape patch is given in Figure 2 (a). To achieve a better performance parameter, a slot of size L1 × W1 has been etched out on the patch, as depicted in Figure 2(b). The various kind of slots are loaded on the patch of the proposed antenna, resulting in two distinct patch structures called Patch-A and Patch -B. Loading slots on the patch enhances the antenna performance parameter. The patch structures A and B are given in Figures 2 (c) and(d). Metamaterial (MTM) is implemented in both Patch-A and Patch-B. For patch structure A the circular shape metamaterial structure has been implemented and the structure is called ANT-A and for patch B the rectangle shape of metamaterial has been added and the structure is called ANT-B. The gain enhancement is achieved after implementation of metamaterial along with the slot loaded patch. In ANT-A and ANT-B the addition of circular MTM and rectangle MTM respectively is depicted in Figure 3(a) and (b). The proposed antenna dimensions are specified in Table 1.

Table 1. Ant-A And Ant-B Dimensions

Dimensions	Value	Dimensions	Value
L	0.941	b	0.1
W	1.683	С	0.19
Lg	5.141	d	0.44
Wg	5.883	e	0.7
S1= S2	1	f	0.28
q1 =q2	1	g	1
Wm= Lm	0.6	h	0.45
Rm	0.28	i	0.3
g1	0.5	j	0.1
g2	0.8	k	0.36
k1	0.383	1	0.37
k2	0.05	m	0.15
d1	0.2	n=s	0.05
d2	0.5	0	0.06
d1'	0.1	p	0.15
d2'	0.6	q	0.26
a	0.33	r	0.1
t	0.1	u=v=w	0.07

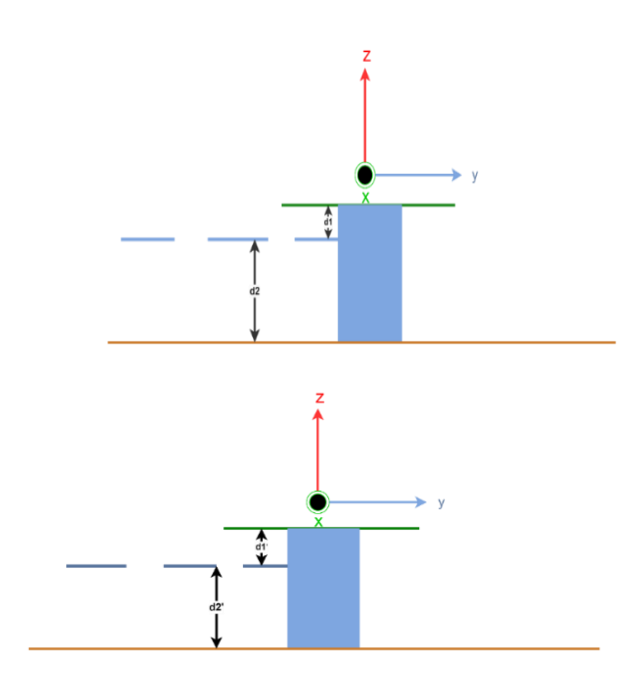
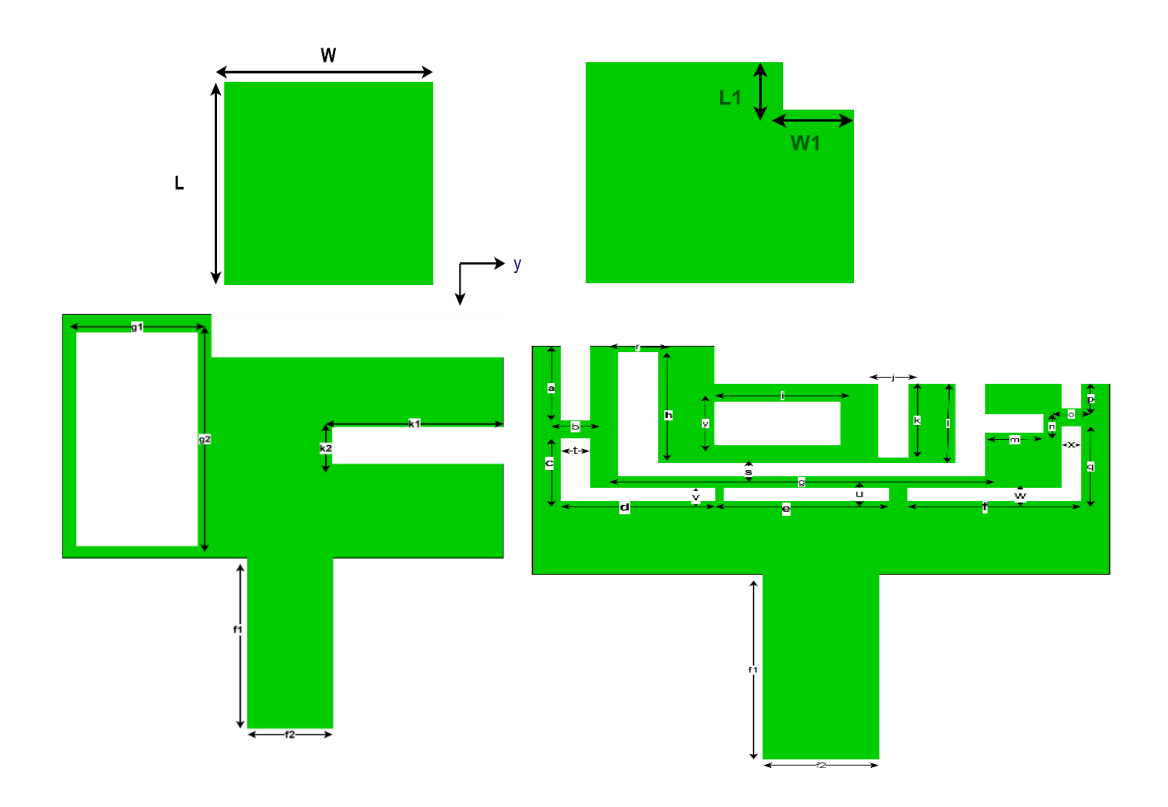
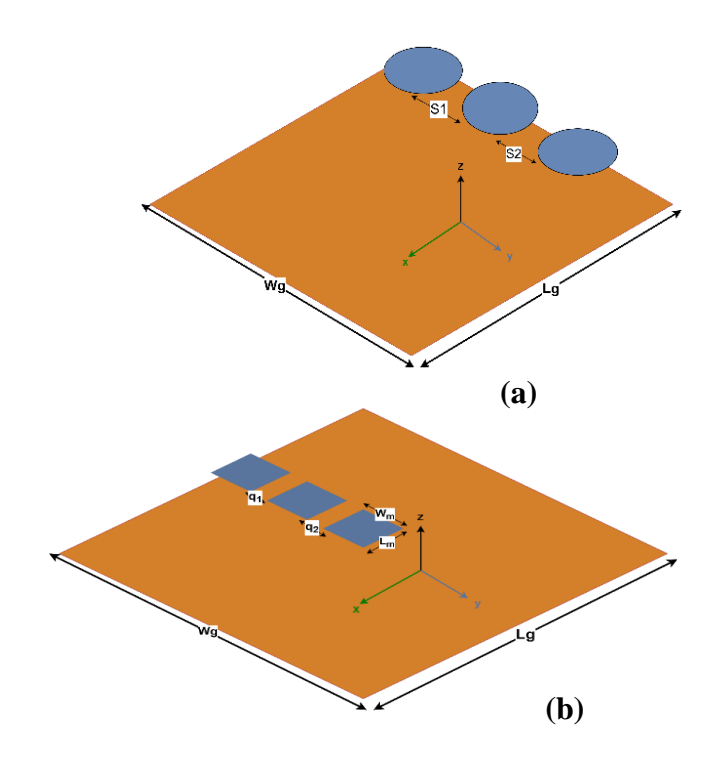


Figure 1. (a) Front View of ANT-A (b) Front View of ANT-B



**Figure 2**. (a) Front View of Simple Patch (b) Front View of Patch with L1×W1 Slot (c) Patch A Structure With Dimensions (d) Patch B Structure with Dimensions



**Figure 3.** (a) Metamaterial Implemented in ANT-A (b) Metamaterial Implemented in ANT-B

### 4. Results and Discussion

In the rectangle shape patch, which has been shown in Figure 2, (a) a rectangle slot of length L1 and width W1 has been etched out. Etching the slots on the rectangular patch changes the antenna performance characteristics. The change in the gain, return loss and axial ratio can be seen in Figure 4 (a), (b), (c). The change in the slot length changes the antenna gain and CP bands. This has been represented in Table 2. From table 2 it can be seen that the gain is maximum for L1=0.9mm at 318.137GHz and the value obtained is 34.1599dBi. The maximum gain value graph with a change in length has been represented in Figure 4(b). For L1=0.9mm the resonating frequencies are 31.379GHz,137.206GHz, and 313.586GHz with the Return loss values are -21.0499dB, -34.719dB, -12.886dB, and the bandwidth covered are (28.3241-33.563) GHz, (35.758-297.512) GHz, (301.457-325.386) GHz which can be seen from Figure 4(a)and the AR<3dB plot has been represented in Figure 4(c). For L1=0.5 the maximum number of CP bands have been achieved but the gain value is 13.97dBi while in the case of L1=0.9 the cp band achieved are 4 but the gain is 29.47dBi. These bands cover the frequency regions are (86.112-88.3668) GHz, (114.304-117.114) GHz, (112.708-124.187) GHz, (and 128.062-128.189) GHz. The change in the W1 is also changing the antenna performance characteristics like return loss, maximum gain value, and cp bands. Which have been given in Table 3, So from Figure 5(b) it can be seen that for different values of W1 the gain is maximum for W1=1.142mm and the maximum gain value achieved is 33.351dBi at the frequency 280.586GHz and the S11<-10dB bands are (29.0652-197.704)GHz,(200.0391-202.1855)GHz, (221.287-222.639) GHz, (234.001-239.980) GHz, (243.803 268.640)GHz,(272.764-280.217) GHz, and (335.174-346.412) GHz which is given in Figure 5(a) and the Axial Ratio graph has been represented in Figure 5(c). The number of CP bands changes with W1 parameter is illustrated in Table 3. With the change in W1, it is observed that for W1=1.242mm, there are 13 CP bands but with a lower gain value of 18.494dBi. On the other hand, for W1=1.142mm, a single CP band is achieved, covering the frequency range (94.694-97.784) GHz, with a higher gain of 33.251dBi.

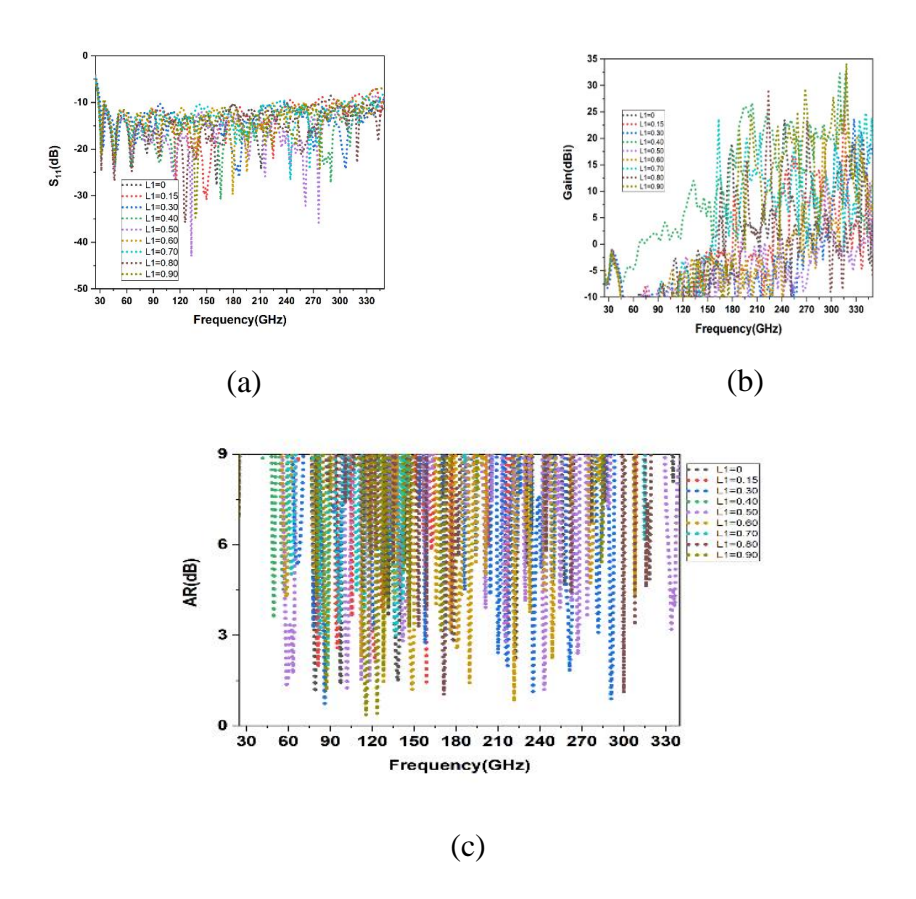
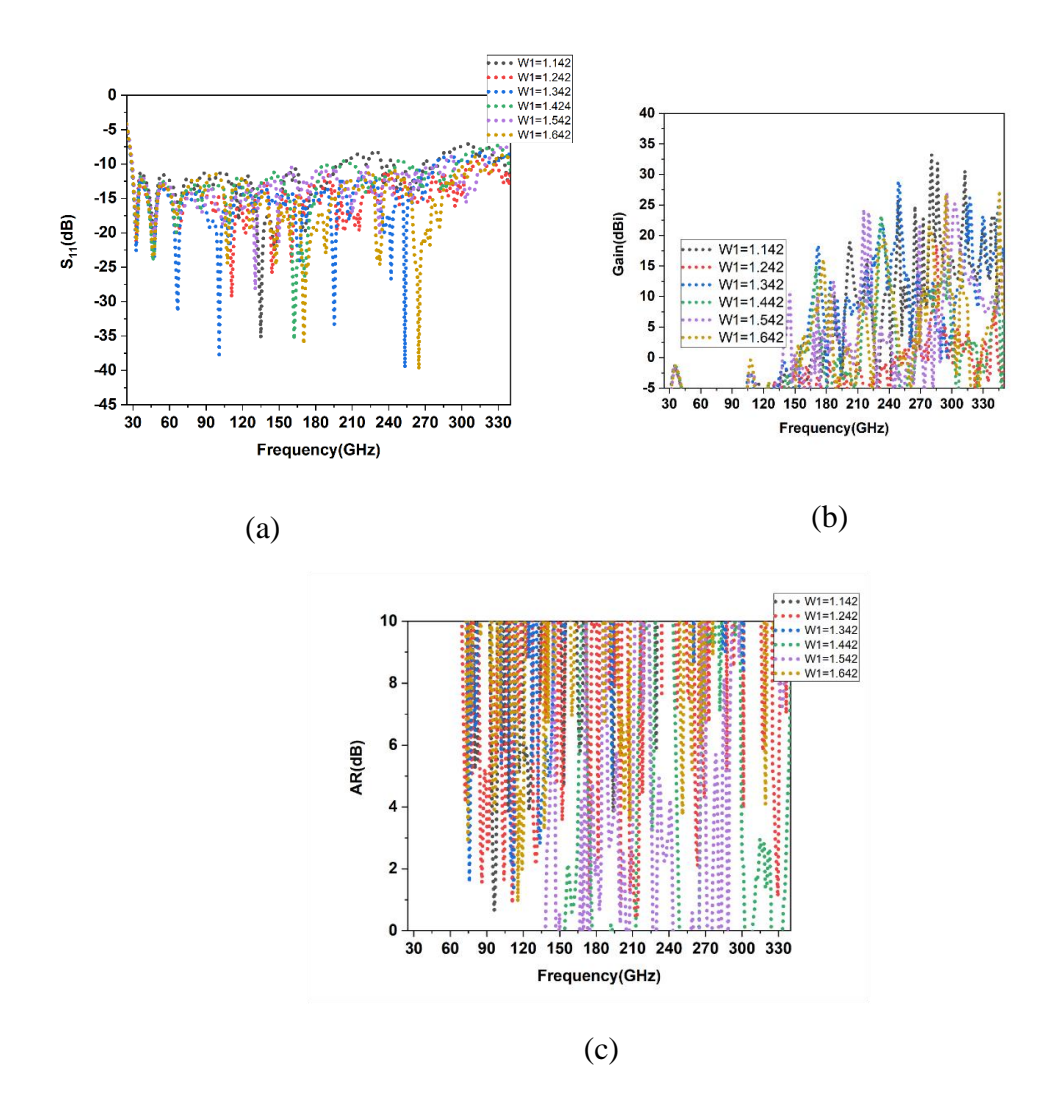


Figure 4. (a)  $S_{11}V/s$  Frequency (b) Gain v/s Frequency (c) AR v/s Frequency for L1

Table 2. Performance Parameter of a Simple Patch with Change in L1

L1	Maximum Gain (dBi)	No. of CP Bands
0	23.536	4
0.15	16.753	4
0.30	23.729	7
0.40	26.684	0
0.50	13.97	10
0.60	21.27	8
0.70	23.711	2
0.80	28.843	3
0.90	29.47	4



**Figure 5.** (a) S<sub>11</sub> v/s Frequency (b) Gain v/s Frequency (c) Axial Ratio v/s Frequency for W1 Variations

Table 3. Performance Parameter of Simple Patch with Change in W1

W1	Maximum Gain (dBi)	No. of CP Bands
1.142	33.251	1
1.242	18.494	13
1.342	28.842	3
1.442	23.285	6
1.542	27.065	3
1.642	26.721	3

### 4.1 ANT-A

After etching the L1×W1, where the L1=0.375mm and W1=1.142mm, two additional slots were etched, resulting in the formation of the Patch-A structure. In the patch-A structure, a maximum gain of 34.257dBi is achieved at the frequency of 232.793GHz. So, cutting the slots of length and width k1, k2, and g1, g2 respectively at the patch is improving the 1dBi in gain. Another performance characteristics axial ratio (<3dB) has been achieved in the frequency range (147.982-150.037) GHz, (140.455-140.8007) GHz, and (96.756-98.0126) GHz. Subsequently, a circular-shaped metamaterial (MTM) was added to Patch-A at a distance of d1=0.2 from the patch. This addition of MTM is improving the antenna characteristics like gain. This can be seen in Figure 7. Ant-A is resonating at 163.379 GHz with an RL value of -25.092dB and the band covered is (28.9974-202.113) GHz. Another resonating frequency is 244.172GHz and the Return loss value is -28.9212GHz covering the band (205.884-336.693) GHz which has been given in Figure 11(a). The maximum gain achieved at 290.827 GHz is 34.759dBi i.e., represented in Figure 11(b) So, the circular MTM structure is increasing the gain slightly and two resonating frequency bands (28.997-202.1131) GHz, (205.889-336.693) GHz have been achieved. In the case of ANT-A, the AR<3dB has been achieved for three frequency bands which are (186.8002-189.105) GHz, (191.151-192.324) GHz, and (132.472-132.8007) GHz which can be seen from Figure 11(c). So as compared to Patch A structure the ANT-A is increasing the gain by 0.5dBi and the three AR<3dB bands are present while in the Patch -A structure only two AR<3dB bands are present. So, the implementation of MTM is improving the antenna performance parameter.

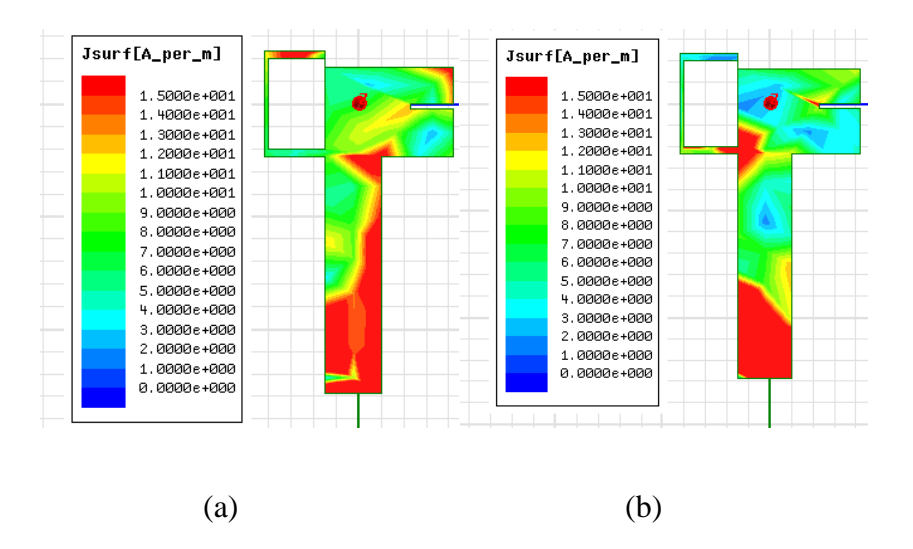


Figure 6. Current Distribution (a) at 163.379GHz (b) at 244.172GHz

### **4.2 ANT-B**

Another patch structure called Patch B is designed by etching different slot structures represented in Figure 2 (d). On the patch, the antenna has a maximum gain value of 33.345dBi at 279.448GHz. This can be seen in Figure 10 (a). For the patch-B structure, the AR versus frequency graph is given in Figure 10 (b). The AR<3dB or circular polarization bands for the patch-B are (290.714-294.713) GHz, and the other bands are (74.738-75.810) GHz and (299.269-299.969) GHz, (334.282-336.484) GHz. In the patch B structure, the MTM structure of the rectangle shape has been added. After the addition of the MTM structure, the structure is ANT-B which is resonating on 171.3448GHz, and 336.3448GHz with the return loss value of -27.865dB, -10.175dB covering the band (29.178-330.486) GHz, (334.936-336.702) GHz. The maximum gain obtained after the implementation of rectangle MTM is 36.3155dBi at the frequency of 299.9310 GHz. This can be seen in Figure 9. Also, the AR<3dB value has been achieved for the bands (80.248-80.358) GHz, (155.209-155.972) GHz, (159.839-160.883) GHz, (161.186-162.331) GHz, (172.1882-173.691) GHz, and (178.1030-178.525) GHz. In the ANT-B the gain is improving by 2.9075 dBi which can be seen in Figure 9 gain plot. Also, the AR <3dB bands in the case of patch -B are 4 while in the case of ANT-B 6 bands are present. So, the implementation of MTM is improving the gain and the CP bands which can be analysed in Tables 4, and 5 also.

**Table 4.** Performance Parameter of the Designed Antenna with the Different Patch Structure

Patch Structure	Maximum gain frequency	Maximum/Peak Gain(dBi)	AR <3dB Bandwidth
Patch A	232.793GHz	34.257dBi	(147.982-150.037) GHz, (140.455-140.8007), (96.756- 98.0126)
Patch B	279.448GHz	33.345dBi	(290.714-294.712) GHz, (74.7335-75.807) GHz, (299.269-299.969), (334.282- 336.484) GHz

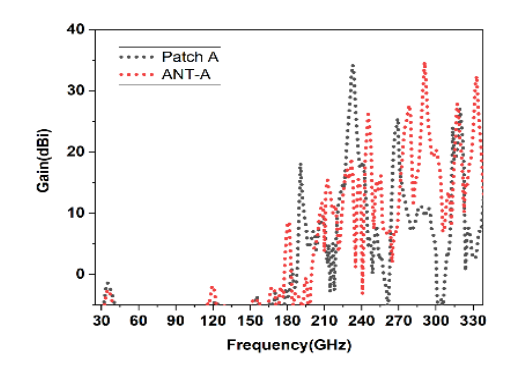


**Figure 7**. Patch A and ANT A Comparative Gain Plot.

**Table 5.** Performance Parameter of the Designed Antenna with the Different ANT Structure

ANT	Resonating	Maximum	RL	AR <3dB Bandwidth
Structure	Frequencies (GHz)	/Peak	Bandwidth	
		Gain(dBi)		
ANT -A	163.379,244.172	34.759dBi	(28.997- 202.1131) GHz, (205.889- 336.693) GHz	(186.8002-189.105), (191.151-192.324) GHz, (132.472-132.8007) GHz.
ANT-B	171.3448GHz,336.344	36.3155dBi	(29.178- 330.486) GHz, (334.936- 336.702) GHz	(80.248-80.358) GHz, (155.209-155.972) GHz, ,(159.839- 160.883)GHz,(161.186- 162.331)GHz, ,(172.1882- 173.691)GHz,(178.1030- 178.525)GHz.

In Table 4, a comparative analysis has been given between patch-A and patch B. Also from Table 5, it can be seen that ANT-A has a maximum gain of 34.759dBi and ANT-B has a maximum gain of 36.3155dBi. So, ANT-B has more gain as compared to ANT-A. Also, the RL bandwidth is 301.308. GHz,1.766GHz at 171.3448GHz and 336.344GHz respectively for ANT-B, and ANT-A is resonating on two frequency bands 163.379GHz, 2.44.17GHz with the bandwidth 173.116GHz,130.804GHz. The AR<3dB bands for ANT-A is at three frequency bands and for ANT-B six frequency bands in which the antenna shows circular polarization property. Also, the comparative analysis of ANT-A and ANT-B return loss, gain and AR is given in Figure 11(a), (b), (c). So, from the given plot, it can be concluded that the ANT-A is resonating on the two frequency bands and the ANT-B also resonates on the two frequency bands but the maximum gain is more in the case of ANT-B as compared to ANT-A. Also, the CP bands are more in ANT-B as compared to ANT-A.

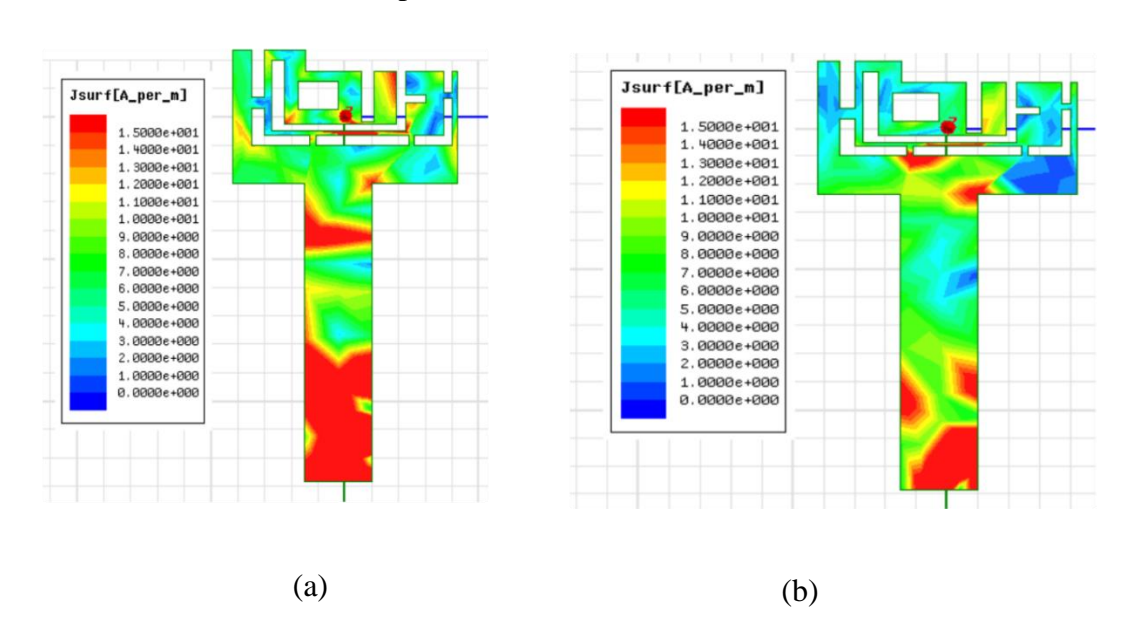


Figure 8. Current Distribution at (a)171.3448GHz (b) 336.3448GHz.

In Figure 6(a) and (b) and Figure 8(a) and (b) the current distribution plot has been given at the resonating frequencies 163.379GHz, 244.172GHz, and 171.3448GHz,336. 344GHz. The current distribution gives information about how the current follows the path on the surface of the antenna. Which has been represented in the current plots for the proposed antenna.

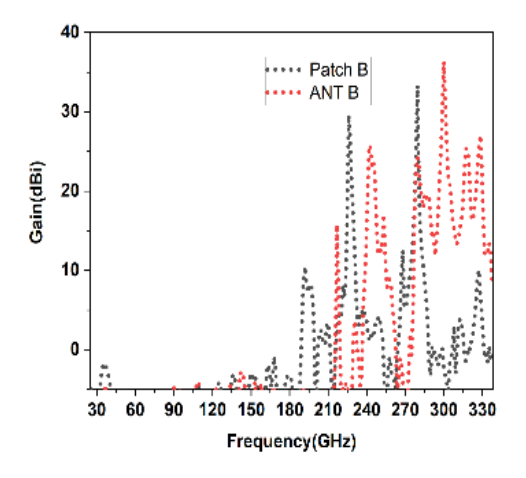
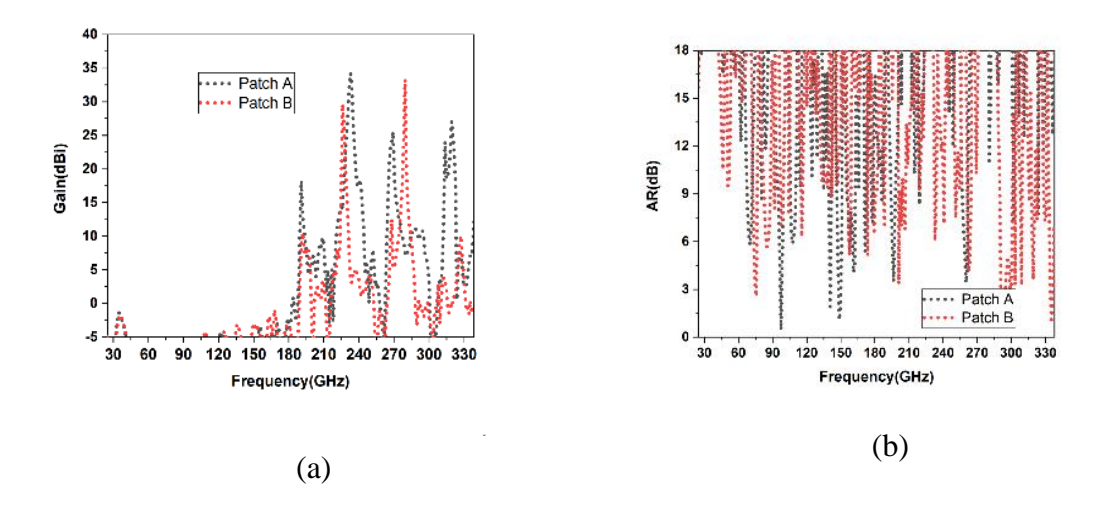
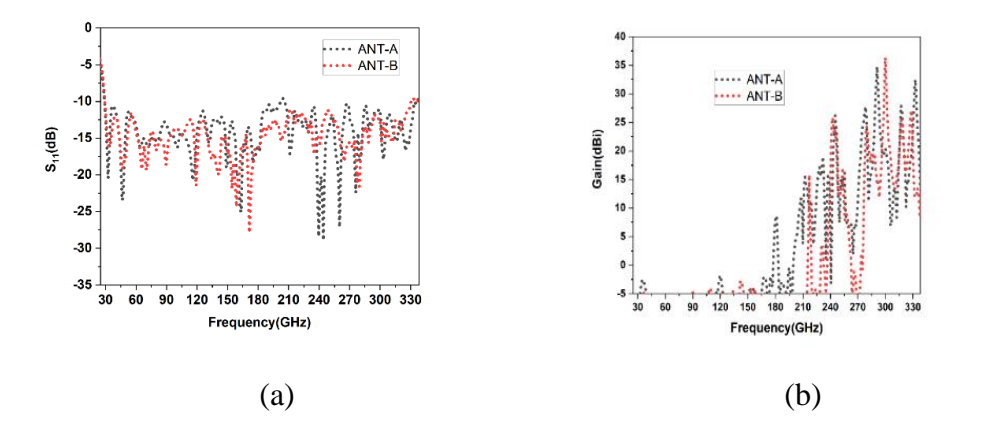
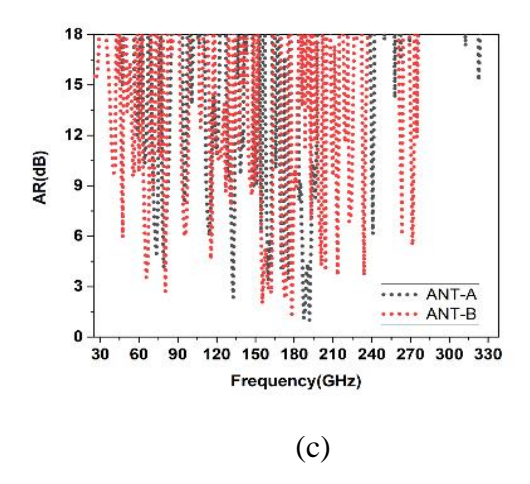


Figure 9. Patch B and ANT B Gain Comparative



**Figure 10.** (a) Gain v/s Frequency Plot (b) Axial Ratio V/s Frequency plot comparative graph for Patch A and Patch B.





**Figure11**. (a)  $S_{11}$  v/s Frequency (b) Gain v/s Frequency (c) AR v/s Frequency Comparative of ANT-A and ANT-B

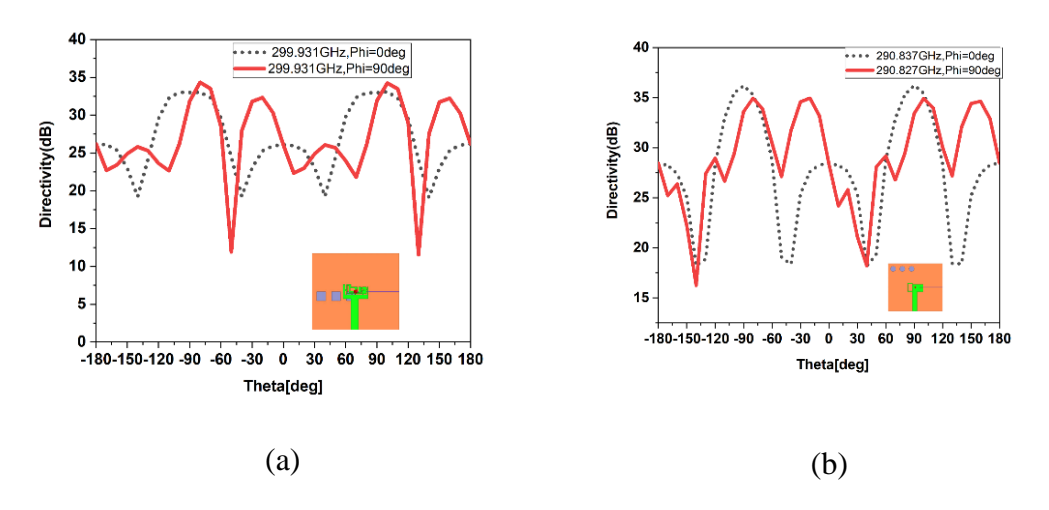


**Figure 12.** (a) Directivity Plot at Frequency 290.837 GHz of ANT-A (b) Directivity Plot at Frequency 299.931GHz of ANT-B.

In Figure 12(a) and(b) the directivity plot of the ANT-A and ANT-B is given. The maximum directivity achieved for ANT-A is 36.2337dBi at 290.837GHz and for ANT-B, the maximum value is 34.342dBi at 299.931GHz. In Table 6 the comparative analysis with the previous literature, has been represented and it can be analyzed that proposed antenna structures, ANT-A and ANT-B, have good maximum gain and dual-band resonating.

**Table 6**. Comparative Analysis with the Previous Literature

References	Maximum gain/Peak gain(dBi)	RLBW
[18]	20.3	(1.02 to 1.08) THz
[19]	12.1	(3.7-4.2) GHz
[20]	21.9	(28–34) GHz
[21]	11.8	(29.1–31.1) GHz
[22]	14.6	(56.0–66.2) GHz
[23]	17.85	(57.2–64.2) GHz
[24]	16.5	(25-34) GHz
[25]	26.1	(55.4 to 66.5) GHz
[26]	18.8	(38-50) GHz
[27]	19.5	(56.55 GHz - 65.13) GHz
[28]	17.7	(282 – 304) GHz
Proposed ANT-A	34.759	(29.0010-202.1152) GHz, (205.884- 336.693) GHz
Proposed ANT-B	36.3155	(29.179-330.486) GHz, (334.936-336.702) GHz

### 5. Conclusion

ANT-A and ANT-B have been designed in the proposed article for mm-wave 5G and Sub-THz communications. ANT-A has been designed by using patch structure A while ANT-B has been designed using patch structure B. The implementation of MTM is improving the antenna performance characteristics. In ANT-A the maximum gain of 34.759dBi has been achieved along with the AR<3dB band for mm-wave and sub-THz frequency bands. The RL bandwidth covers two resonating frequencies, 163.379 GHz and 244.172GHz that is 173.116GHz and 130.804GHz. Similarly, in the ANT-B the maximum gain of 36.3155dBi is

achieved, and AR<3dB is achieved for mm-wave and Sub-THz bands along with RL bandwidth of 301.308GHz,1.766GHz at the resonating frequencies 171.3448GHz and 336.3155GHz. The designed ANT structures are simulated on HFSS software. The high gain with the CP polarization has been achieved for mm-wave and sub-THz bands, along with the compact structures, and is useful for mm-wave 5G and sub-THz communication.

### References

- [1] Das, P. Chowdhury, A. Biswas, P. Pratim Sarkar, and S. Kumar Chowdhury, "Analysis of a Miniaturized Multiresonant Wideband Slotted Microstrip Antenna with Modified Ground Plane", *IEEE Antennas and Wireless Propagation Letters*, 14 (2014): 60-63
- [2] R. Yazdani, H. Aliakbarian, A.Sahraei, Guy A. E. Vandenbosch, "A compact triple-band dipole array antenna for selected sub 1 GHz, 5G and WiFi access point applications", *IET Microwaves, Antennas & Propagation*, 15, no. 15 (2021): 1866-1876.
- [3] K. Wei, J.L. Wang, R. Xu, Xia Ai, "A new periodic fractal parasitic structure to design the circularly polarized microstrip antenna for the satellite navigation system", *IET Microw. Antennas Propag.* 15, no. 15 (2021): 1891-1898.
- [4] J. Wang, Fan Wu, D. Jiang, Y. Li, "Wideband end-fire circularly polarized complementary source antenna for millimeter-wave applications", *IET Microw*. *Antennas Propagation*, 2021;15:1936–1944.
- [5] C. Zhang, Longye Li, R. Zhang, Y. Shao, Feng Lin, "A single-microstrip-fed S-shaped magneto-electric dipole array with broadband circular polarization for MMW applications", *IET Microw. Antennas Propag.* 2021;15:1743–1753.
- [6] M. Midya, A. Ghosh, M. Mitra, "Meander-line-loaded circularly polarized square-slot antenna with inverted-L-shaped feed line for C-band applications", *IET Microw*. *Antennas Propag*. 2021;15:1425–1431.
- [7] Q. Zeng, Z. Xue, W. Ren, W. Li, S.Yang, "A high-gain circular polarization beam scanning transmit array antenna, *IET Microw. Antennas Propag.*", 2021;15:1519–1528.

- [8] A. Ghalib, M S. Sharawi, R. Mittra, H. Attia, A. Shammim, "Collocated MIMO traveling wave SIW slot array antennas for millimeter waves", *IET Microw. Antennas Propag.* 2021;15:815–826.
- [9] J.R. Reis, C. Ribeiro, R F. S. Caldeirinha, "Compact 3D-printed reflector antenna for radar applications at K-band", *IET Microw. Antennas Propag.* 2021;15:843–854.
- [10] A.M. Eid, A. A. Salama, H. M. Elkamchouchi, "A novel circularly polarized slotted substrate integrated waveguide antenna array for satellite applications", *IET Microw.*, *Antennas Propag.* 2021; 15:925–936.
- [11] B. Feng, J. Chen, C.Y.D. Sim, "Analysis of double-Xi-shaped millimeter-wave patch antenna backed by a high-order-mode cavity using characteristic mode design", *IET Microw. Antennas Propag.* 2021;15:966–980.
- [12] H.Y. Yu, J. Yu, Y. Yao, X. Liu, X. Chen, "Wideband circularly polarized horn antenna exploiting open slotted end structure", *IEEE Antennas and Wireless Propagation Letters*, 19, no. 2 (2020): 267-271.
- [13] Y. Yang, B.H.Sun and Jing-Li Guo, "A Low Cost, Single-Layer, Dual Circularly Polarized Antenna for Millimeter-Wave Applications", *IEEE Antennas and Wireless Propagation Letters*, 18, no. 4 (2019): 651-655.
- [14] X. Ruan, S.W. Qu, Q. Zhu, K. B. Ng, and C. H. Chan, "A Complementary Circularly Polarized Antenna for 60-GHz Applications", *IEEE Antennas and Wireless Propagation Letters*, 16 (2016): 1373-1376.
- [15] Z. Liu, P. Wang, and Z. Zeng, "Enhancement of the Gain for Microstrip Antennas Using Negative Permeability Metamaterial on Low-Temperature Co-Fired Ceramic (LTCC) Substrate", *IEEE Antennas and Wireless Propagation Letters*, Vol. 12, 2013 429-432.
- [16] I. Mohamed, and A. Sebak, "60-GHz 2-D Scanning Multibeam Cavity Backed Patch Array fed by Compact SIW Beam-Forming Network for 5G Applications", *IEEE Transactions on Antennas and Propagation*, 67, no. 4 (2019): 2320-2331.
- [17] Y.F. Lin, W.C. Chen, C.H. Chen, C.T. Liao, N.C. Chuang, and H.M. Chen, "High-Gain MIMO Dipole Antennas with Mechanical Steerable Main Beam for 5G Small Cell",

- *IEEE Antennas and Wireless Propagation Letters, Vol.* 18, NO. 7, JULY 2019 1317-1321.
- [18] S.Y. Zhu, Y.L. Li, K.M. Luk, and S. W. Pang, "Compact High-gain Si-imprinted THz Antenna for Ultra-high Speed Wireless Communications", 3, *IEEE Transactions on Antennas and Propagation*, 68, no. 8 (2020): 5945-5954.
- [19] J.D Ntawangaheza, C. Yang, Y. Pang, and G. Rushingabigwi, "Thin Profile Wideband and High Gain Microstrip Patch Antenna on a Modified AMC", *IEEE Antennas and Wireless Propagation Letters*, 18, no. 12 (2019): 2518-2522.
- [20] Y.H. Yang, B.H. Sun, and J.L. Guo, "A Single-Layer Wideband Circularly Polarized Antenna for Millimeter-Wave Applications", IEEE *Transactions on Antennas and Propagation*, 68, no. 6 (2019): 4925-4929.
- [21] Y.H. Yang, B.H. Sun and J.L. Guo, "A low cost, single-layer, dual circularly polarized antenna for millimeter-wave applications," *IEEE Antennas Wireless Propag.* Lett., vol. 18, pp. 651–655, 2019.
- [22] D. J. Bisharat, S. Liao, and Q. Xue, "High gain and low cost differentially fed circularly polarized planar aperture antenna for broadband millimeter-wave applications," *IEEE Trans. Antennas Propag.* vol. 64, no. 1, pp. 33–42, Jan. 2016.
- [23] J. Zhu, S. Liao, Y. Yang, S.Li, and Q. Xue, "60 GHz dual-circularly polarized planar aperture antenna and array", *IEEE Trans. Antennas Propag.*, vol. 66, no. 2, pp. 1014–1019, Feb. 2018.
- [24] Y.H. Yang, S.G. Zhou, B.H. Sun, and X.Z. Gao, "Design of Wideband Circularly Polarized Antenna Array Excited by Substrate Integrated Coaxial Line for Millimeter-Wave Applications", *IEEE Transactions on Antennas and Propagation*, 69, no. 12 (2021): 8943-8948.
- [25] Y. Li and K. Luk, "A 60-GHz wideband circularly polarized aperture-coupled magnetoelectric dipole antenna array," *IEEE Trans. Antennas Propag.*, vol. 64, no. 4, pp. 1325– 1333, Apr. 2016

- [26] Z. Gan, Z. Tu, Z. Xie, Q. Chu, and Y. Yao, "Compact wideband circularly polarized microstrip antenna array for 45 GHz application," *IEEE Trans. Antennas Propag.*, vol. 69, no. 11, pp. 6388–6392, Nov. 2018.
- [27] Q. Zhu, K. Ng, and C. H. Chan, "Printed circularly polarized spiral antenna array for millimeter-wave applications," *IEEE Trans. Antennas Propag.*, vol. 65, no. 2, pp. 636– 643, Feb. 2017.
- [28] B. Aqlan, M. Himdi, H. Vettikalladi, & Laurent Le-Coq, "A 300-GHz low-cost high-gain fully metallic Fabry–Perot cavity antenna for 6G terahertz wireless communications", *Scientific Reports*, 11, no. 1 (2021): 7703.

## Author's biography

**Author Name** -Aafreen Khan has completed her B. tech from Jamia Millia Islamia with overall CGPA of 9.04 and had completed her M. tech from Jamia Millia Islamia with overall CGPA of 9.6. and doing her PhD from jamia millia islamia.

**Second Author Name** -Anwar Ahmad is professor of jamia millia islamia in the department of Electronics and Communication New Delhi.